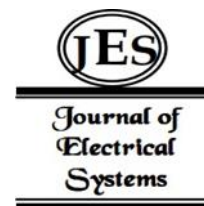


<sup>1</sup>Muneeb Ahmad<sup>2</sup>K. A. Dongre

## Solar Photo Voltaic Connected Quasi Z Source Inverter for Grid and utility Application



**ABSTRACT:** This paper discusses the use of quasi-Z-source inverters, in utility grid systems. These inverters enhanced dependability and one-stage buck and boost abilities make them appropriate for photovoltaic power conditioning applications. The small signal state space method utilized for the proposed system using Quasi ZSI for utility and grid integration application. Shoot through state also implemented on dc side to enhanced the voltage gain. The Controlling of dc side and ac side also implemented in MATLAB using state space transfer function. A two-stage controlling technique implemented on two level 6 switch inverters with SPWM with P & O MPPT and PI controller. The proposed system has solar PV array rating of 5.5kW and utilized in distribution purpose. A simple boost controlling technique has been implemented to obtained the desired gain and less ripples are present in the current due to the presence of inductor in the QZSI impedance network. During light loading the surplus power injected to the grid with the help of PLL system and when load demand increases the power take from the grid smoothly without loss of synchronism. The system has better stability and fast dynamic response during transient. The THD has been observed at the inverter and load side with LC filter, THD within the permissible limit as per IEEE std 1547.

**Keywords:** Quasi impedance source inverter, sine pulse width modulation, shoot through, duty ratio, Grid, photo voltaic, perturb & observed, total harmonic distortion (THD).

<i>ZSI</i>	<i>Impedance Source inverter</i>	$T_1$	<i>non-shoot-through interval</i>
<i>MPPT</i>	<i>Maximum power point tracker</i>	$d_0 = T_0/T_s$	<i>shoot-through duty ratio</i>
<i>QZSI</i>	<i>Quasi impedance source inverter</i>	$D_0$	<i>Steady state duty ration</i>
<i>SPWM</i>	<i>Sinusoidal Pulse-Width Modulation</i>	<i>FFT</i>	<i>Fast Fourier transformation</i>
$i_{L1}$ & $i_{L2}$	<i>series inductor current in ampere</i>	$K_P$	<i>Proportional gain of PI controller</i>
$M$	<i>Modulation index</i>	$K_I$	<i>Integral gain of PI controller</i>
$v_{C1}$ & $v_{C2}$	<i>Capacitor voltage</i>	$I_{load}$	<i>Load Current</i>
$r = r_1 = r_2$	<i>stray resistances of inductors</i>	<i>P&amp;O</i>	<i>Perturbation and Observation</i>
$R = R_1 = R_2$	<i>series resistances of capacitors</i>	<i>THD</i>	<i>Total harmonic distortion</i>
$T_0$	<i>shoot-through interval</i>	<i>PCC</i>	<i>Point of common coupling</i>

<sup>1</sup>Department of Electrical Engineering, Piyadarshini College of Engineering, Nagpur, India (muneebelco@gmail.com)

<sup>2</sup>Department of Electrical Engineering, Prof. Ram Meghe Institute of Engineering & Management, Badnera Amravati, India (kirandongre2015@gmail.com)

Copyright © JES 2024 on-line : journal.esrgroups.org

### I. INTRODUCTION

Power electronic converters, such as Z-Source Inverters, play a critical role in facilitating the interface between dispersed power grids and renewable energy sources[1][2], [3]. Z-Source Inverters offer several benefits, including enhanced voltage output, flexibility, and reliability, making them suitable for various applications where these characteristics are essential. Z-Source Inverters stand apart from traditional capacitor-based networks through the integration of a unique impedance network, known as the Z-network[1][3], [4]. This innovative design feature offers several advantages, including heightened resilience against input power fluctuations and enhanced control over power flow. By leveraging the Z-network, Z-Source Inverters can effectively regulate and stabilize the input voltage, ensuring consistent performance even in dynamic operating conditions. This capability not only enhances the reliability and efficiency of the inverters but also enables more precise management of power transfer, contributing to greater flexibility and control in diverse applications.[3], [5]. To overcome various constraints linked with traditional Z-Source Inverters, scholars have introduced the Quasi-Z-Source Inverter. (QZSI)[4], [6]. Similar to its predecessor, the QZSI converts direct current (DC) to alternating current (AC) and offers advantages such as continuous input current, voltage enhancement, and increased dependability[4][7].

The field of Quasi-Z-Source Inverters is continuously evolving, with engineers and researchers working to improve efficiency and expand the range of applications in various power system scenarios. Studies suggest the implementation of a two-stage control scheme for an asymmetric quasi-Z-source network to enhance system properties and ensure steady capacitor voltage for connecting renewable energy sources to distributed power grids[4], [6][3].The integration of Quasi Z Source Inverters in solar photovoltaic systems holds immense potential for advancing clean energy generation and enhancing grid performance[3]. Continued research and development in this field will further optimize the efficiency and reliability of power conversion technologies, supporting the transition towards sustainable energy solutions[3][8].

This paper arranges as chapter-II circuit analysis of quasi ZSI, chapter-III voltage at capacitor, chapter-IV two stage configuration of QZSI for grid connected system. Chapter-V simulation result and then conclusion.

### II.CIRCUIT ANALYSIS OF QUASI-ZSI

The correlation between  $v_{in}$  and  $i_{in}$  is profoundly impacted by the characteristics of the designated energy origin.  $V_{in}$  acts as a pivotal link between the energy source and the system, furnishing invaluable insights into system performance and efficiency[3]. It facilitates comprehension of the input current prerequisites, thereby enabling the optimization of the overall system configuration for peak efficiency. In the realm of the modeling of the DC side for a three-phase inverter bridge and an external AC load, a simplified representation includes a solitary switch and a parallelly connected current source. This configuration is commonly employed to analyze the behavior of the system, offering a convenient way to understand the interplay between the switch, current source, and the overall power conversion process[3], [9]. This simplification streamlines the modeling procedure and enables a more precise evaluation of the system's functionality. Concentrating on the DC aspect of the inverter empowers engineers to fine-tune the system for heightened efficiency and effectiveness[3], [9]. Grasping the nuances of input voltage and its interplay with input current is imperative for comprehensive system scrutiny and modeling. By integrating input voltage parameters into the DC-side modeling of three-phase inverters, engineers can elevate both the efficiency and performance of the system. In essence, input voltage assumes a pivotal role in refining system design and guaranteeing optimal energy utilization[2], [3], [10].

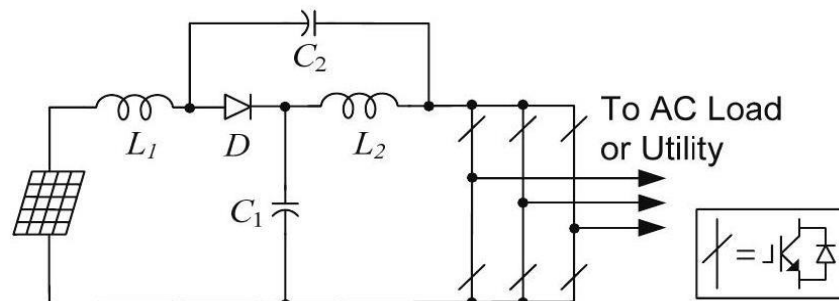


Fig1. SPV quasi-Z-source inverter

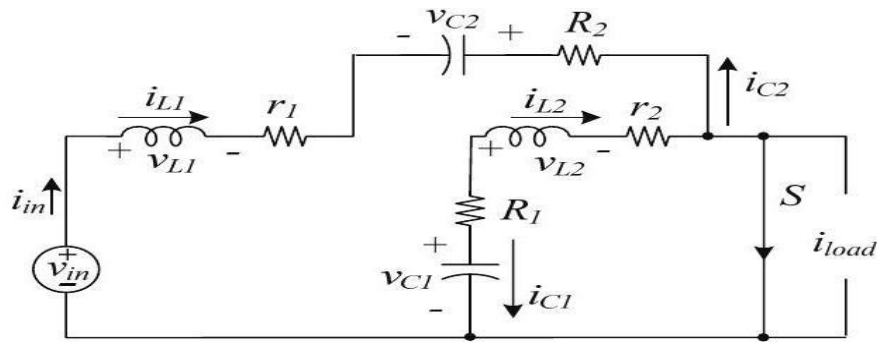


Fig.2 a. Quasi-Z-source inverter during shoot through state

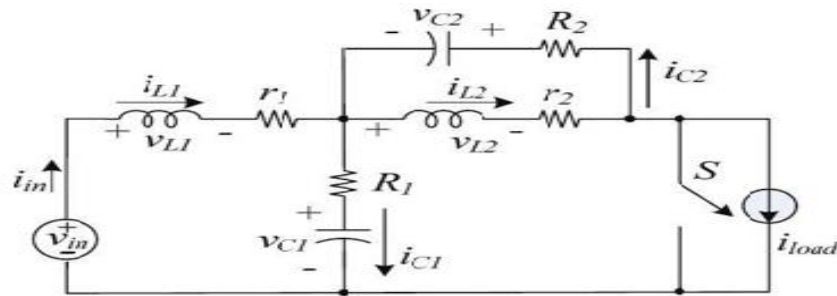


Fig.2 b. Quasi-Z-source inverter during non-shoot through state

To comprehend the operation of a quasi-Z-source inverter thoroughly, a meticulous examination of the various state variables in play is imperative, along with an assessment of the impacts of both shoot-through and non-shoot-through states on the circuit's operation are significant for overall energy conversion process. [2][3]. As depicted in figure.2 (a) & (b).

### III.VOLTAGE AT CAPCITOR

Due to the single buck-boost capability of Quasi Z-source inverters (QZSI), the duty cycle ( $d_0$ ) and modulation index ( $M$ ) are interdependent, making controller design challenging. When  $D_0$  is high,  $M$  tends to be small, and conversely, when  $D_0$  is low,  $M$  increases[3], [11]. This relationship between  $D_0$  and  $M$  complicates controller design and necessitates careful consideration during system optimization. Moreover, this interdependence can lead to increased stress on switching devices due to the requirement for high-rated components. The relationship between  $D_0$  and  $M$  is illustrated in Table 1. Comparing different boosting methods based on modulation index, duty ratio, and peak-to-peak capacitor voltage sheds light on their respective advantages and drawbacks. In the case of QZSI, voltage boost is achieved by partially or completely substituting conventional zero states (000 or 111) with shoot-through states while keeping the six active states unchanged has notable implications. [2], [3], [12]. This unique approach to boosting voltage in QZSI influences the modulation index ( $M$ ) and duty cycle ( $D_0$ ), as well as the peak-to-peak capacitor voltage, contributing to its distinctive performance characteristics compared to other boosting methods[13], [14].To prevent overlap between the duty cycle ( $d_0$ ) and modulation index ( $M$ ), In most Distributed Generation (DG) applications, It is noted capacitor C1 generally maintains a level exceeding twice the peak output voltage considering that the peak output voltage ( $V_{p\_peak}$ ) typically remains constant in such scenarios, regulating the capacitor voltage to a consistent value despite input fluctuations becomes achievable. Within a closed-loop control system, the maintenance of a minimum capacitor voltage facilitates achieving minimum  $d_0$  and maximum  $M$  values inherently. Consequently, this minimizes voltage stress across devices, thereby enhancing the overall reliability and efficiency of the system. Effectively regulating the capacitor voltage allows for the optimization of the quasi-Z-source inverter's operation while ensuring stable performance under varying load conditions.[2], [3], [12].Fig.4 illustrates a two-stage control method for grid-connected q-ZSI, highlighting the significance of this control strategy in managing the inverter's operation effectively within a microgrid environment. The proposed model as shown in figure.3 consist of solar string as source and QZSI as a link between utility and source. QZSI has the impedance network consists of two inductors and two capacitors connected in a specific configuration in such a manner that there is a possibility of energy storing and releasing during non-shoot through and shoot through states. A diode switch is connected to obtain this condition very carefully impedance network provide input to the 3-phase VSI bridge inverter[3], [15]. A L-C filter is used to reduce the harmonics are connected after the inverter but before the utility. This L-C filter minimizes the THD present in the power so that power quality, less distortion and fluctuation in the load which should be maintained as per IEEE std 1547 which will be below 5%. To demonstrate steady state and transient operation load is connected via circuit breaker1 and 2. The load and grid is connected through a point of common coupling for protection and stability point of view[3].

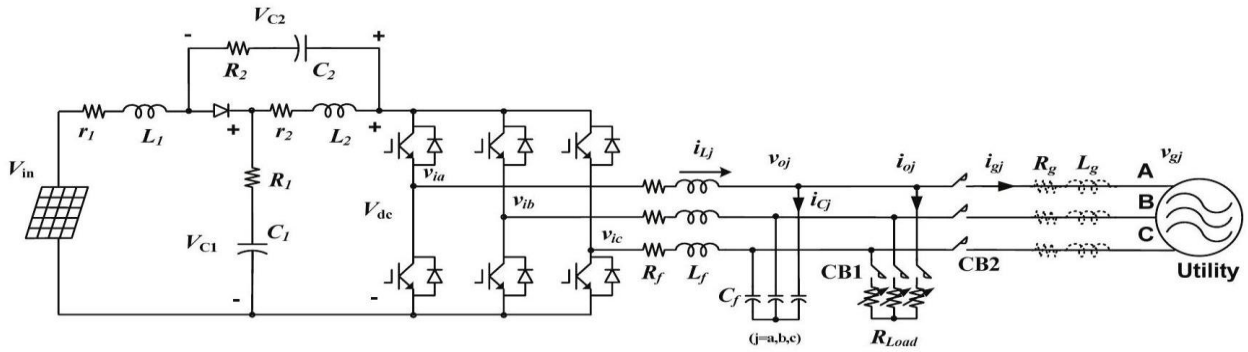


Fig.3. System configuration of the proposed q-ZSI for Grid connected system

#### IV. TWO STAGE CONFIGURATION OF q-ZSI FOR GRID CONNECTED SYSTEM

At the ac side the capacitor voltage which is calculated is returned back to the summing point through capacitor error signal voltage. The grid current amplitude is generated with the help of proportional-integral controller[3]. The condition for injecting the current into the grid is that reference voltage and capacitor voltage difference must be positive. Hence it is essential constant capacitor voltage. The phase locked loop maintains the voltage phase angle of the grid and the reference current combine with PLL signal and  $i_{gj}$  is generated[3]. Ultimately  $v_{ij}$  reference signal compared to triangle wave signal and SPWM generated for inverter switches. In small signal mode the grid current and load current are proportional. This relation describes equation (4) in appendix [3]. The ac side controlling is described in equation (3) which indicates the transfer function iload and capacitor voltage.  $v_{in}^*$  is maintained by MPPT controlling of P & O algorithm by controlling  $d_0$ . For shoot through controlling PI controller is used by controlling  $d_0$  as prescribe in equation (2) the inductor can be altered by varying  $d_0$  which is delivered to input through RES impedance[2], [3], [5], [16], [17].

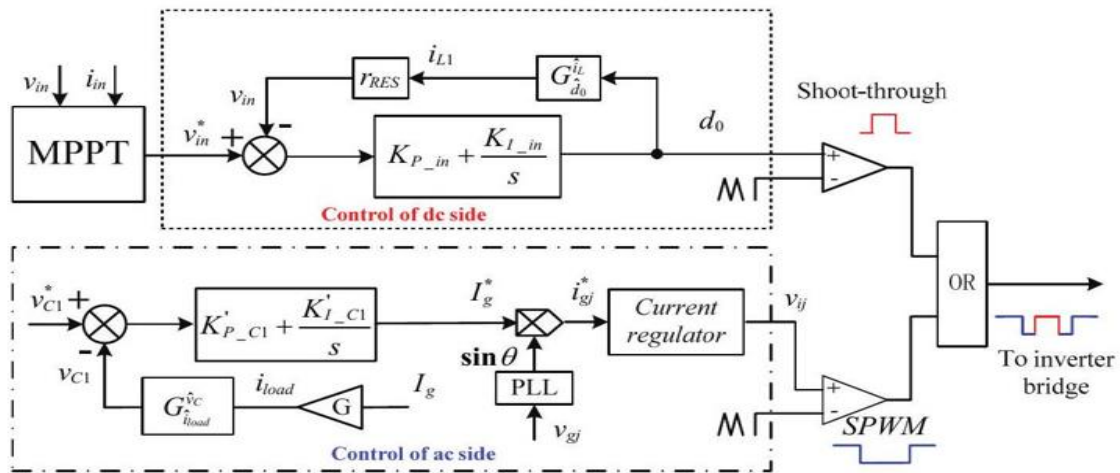


Fig. 4. Solar PV two-stage control method for grid-connected QZSI

Table.2. Solar Module rating (SunPower SPR-305F-WHT-D)

Parameters	Specification
PV Array Model	SunPower SPR-305 E-WHT-D
Parallel String	02
Maximum Power (Pmp)	305.226 W
Open circuit voltage (Voc)	64.2 V
Voltage at maximum power (Vmp)	54.7 V
Cell per modules (Ncell)	96
Short circuit current (Isc)	5.96 A
Current at maximum power point (Imp)	5.58 A
Temp Cell (deg.c)	[0 25 50]
Total Current (Ispv)	11.16 A
Total Voltage (Vspv)	492.3 V
Total Power rating of Solar	5.494 kW

Table.3. Design Parameters of the of q-ZSI used in simulation

Parameters	Specifications
Series inductors $L_1 = L_2 = L$	500 $\mu$ H
Capacitors $C_1 = C_2$	400 $\mu$ F
Inductor resistance	$r = 0.47\Omega$
Capacitor resistance	$R = 0.03\Omega$
Duty ratio ( $D_0$ )	0.1 to 0.4
Load current	9.9 A
Cross-over frequency ( $F_c$ )	10 kHz
Switching Frequency ( $F_s$ ) of IGBT	5 kHz
Natural frequency ( $F_n$ )	50 Hz
Reference Voltage ( $V_{reference}$ )	400 V

### V.SIMULATION RESULTS and Discussion

#### QZSI with P&O and SinPWM

##### Solar PV Array Output

The fig.5. shows the output voltage  $V_{spv}$ , output current  $I_{spv}$  and outpower  $P_{spv}$  has been analyzed and verified with solar PV ratings as per proposed specification of solar PV array. The results of solar output in this system based on 1000 w/m<sup>2</sup> and at temperature of 25 deg-c.

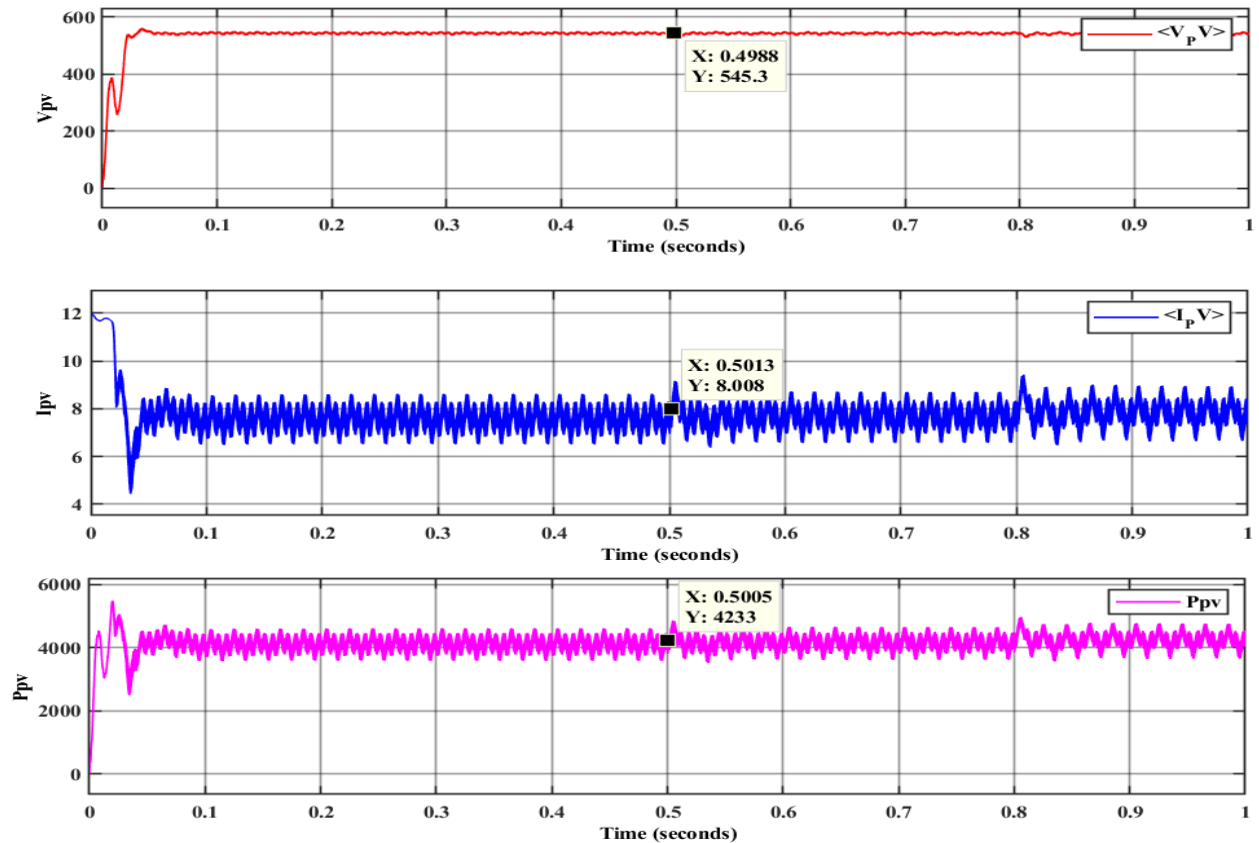


Fig.5.Output of Solar PV Array

The power from solar PV array was 4.23 kW, with PV voltage of 545.3 Volts and current was 8 A at 0.5 second which was as per the solar array rating. The power rating of solar panel was 5.5 kW. Which indicates that P&O algorithm works effectively for tracking maximum power and has extracted maximum power from solar panel.

#### DC Link Voltage

The dc link voltage is provided to voltage source inverter which transform into ac voltage. It has been analyzed that at t=0.5 sec the output voltage from solar panel was 547 volts which has boost up-to 1.44 times the input voltage from solar array hence we can say that system has work with simple boost and converted to 790.9 volts stable output. This is a dc link voltage fed to the six-switch inverter. Figure.6 shows the S1 switch with shoot through pulse and duty ratio of 0.2.

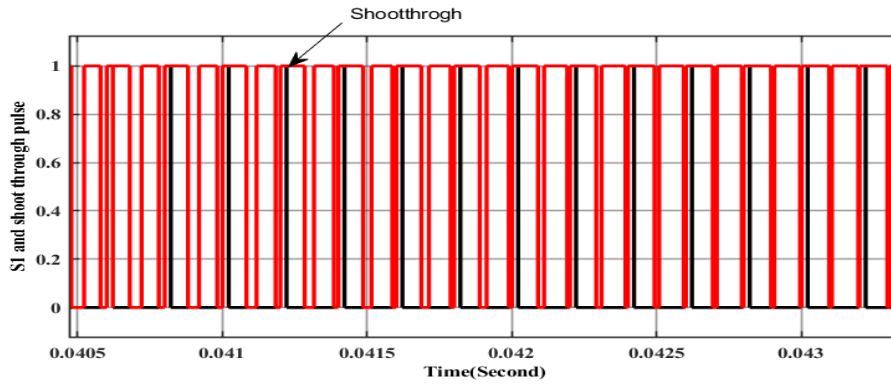


Fig.6.S<sub>1</sub> and shoot through pulse

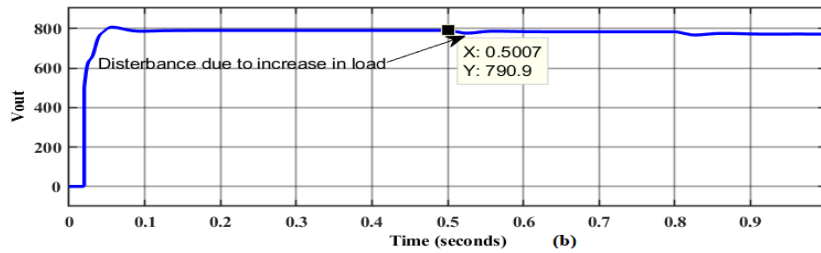
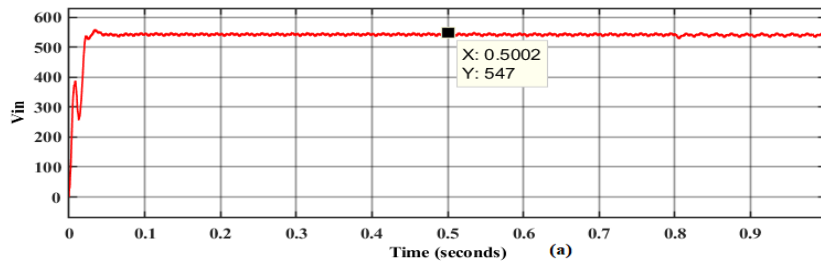


Fig. 7 (a) Input Voltage (b) Output voltage dc link

**Inverter Output Analysis**

The inverter output voltage and current are depicted in Figure 8. The frequency of the inverter switches is 5 kHz. The power injected by the inverter to the LC filter which reduces the THD in the obtained waveform which will improve the power quality. The rating of the inverter decided by a factor of 1.25 to the total input power received by the inverter from dc linked. The output of the voltage of three phase inverter  $V_{abc}$  at time  $t=0.5$  sec was 1238 peak to peak volts which will be sufficiently more than the grid voltage of distribution system (400 Volts phase to phase). The output current of the inverter 21.65 ampere was observed during the simulation.

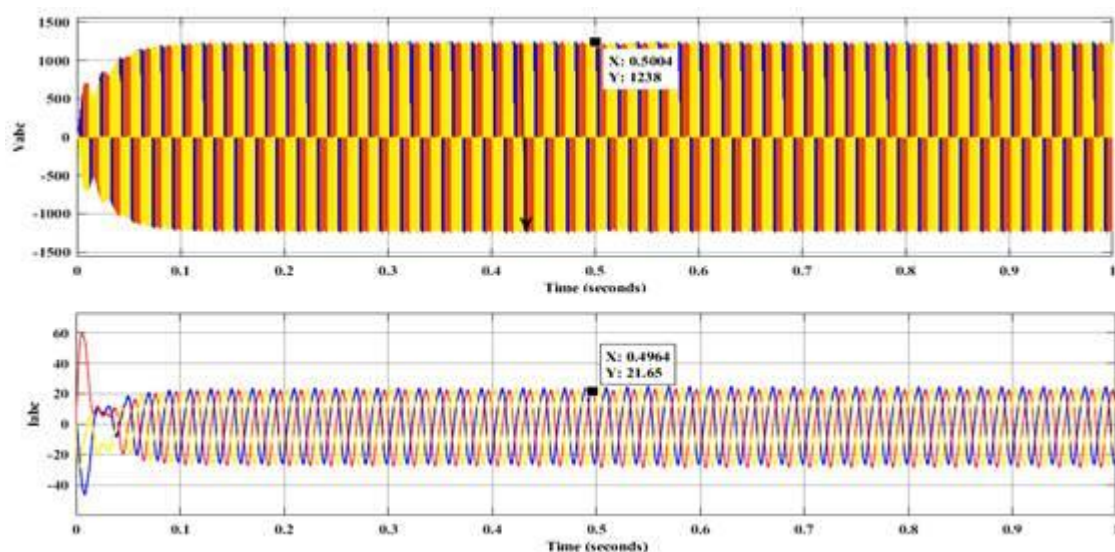


Fig.8 Output of inverter (a) Three phase voltage (b) Three phase current



### Analysis of Output at Load Side

Load voltage and current waveforms at the load side during normal state depicted in fig.9. Under steady state condition and transient condition. At normal condition load voltage and current profile is under within the limit. But when the load demand increases the power requirement has been fulfil by the grid. The voltage profile remains constant and voltage is regulated as per the load requirement. Hence it has been concluded that the system has very quick response and performance has been improving and better reliability and stability of the system, which are crucial factors that determine its performance and operational integrity. When the system runs normal condition the output voltage at load side was 360 rms volts which is under the limit and corresponding load current was 5.45 ampere at light loading (2 kW) up to 0.5 seconds. When the load requirement increases up to 4 kW power the load voltage remains stable 360 rms volts which we required. Hence to full fill load demand some power is taken from grid. From these results we can say that load voltage remains unchanged during transient condition as depicted in figure 9. when load has been increased. The system load voltage has better voltage stability which required for distribution utility. In this way power quality has been enhanced by using Quasi ZSI which shows the appropriateness topology of solar PV converter. Fig.10 shows the active and reactive power demand during normal and abnormal conditions of load. Grid power shows negative up to 0.5 sec it indicates that power is absorbed by grid, after that when load increases power fed to the load through grid and then gride power becomes positive as depicted in figure 11.

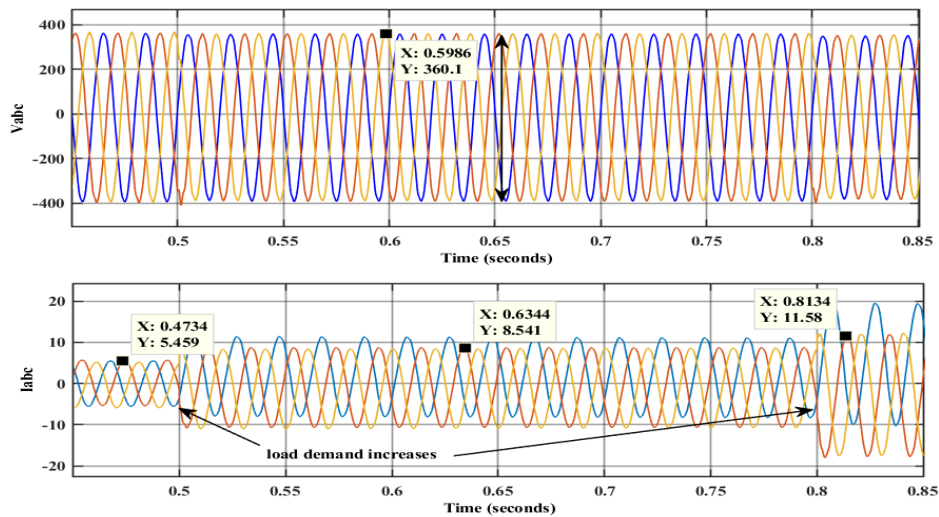


Fig.9. Voltage and current under loading conditions

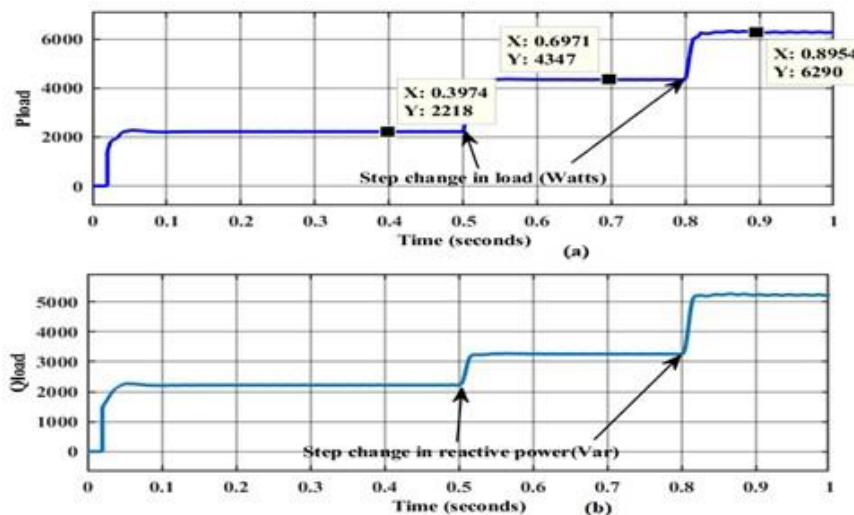


Fig.10 Load side (a) active power (b) reactive power

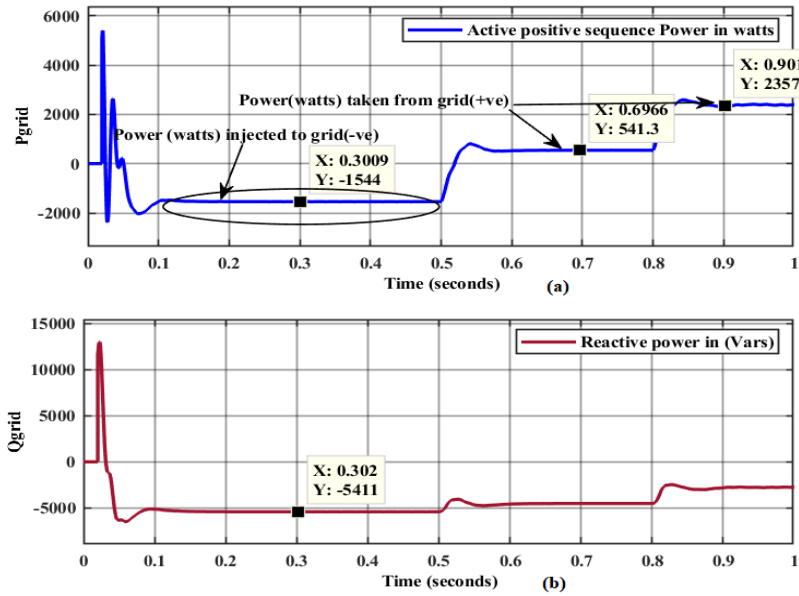


Fig.11 Load side (a) active power (b) reactive power  
**THD Analysis of Voltage and Current Waveform at the Inverter output**

Using Fourier analysis waveform into its harmonic contents. components. The THD content in the load current waveform average value 3.35%. and voltage waveform 4.34% using LC filter. The THD levels for all three phases are within acceptable limits for the intended application as per IEEE std. 1547 (5%).

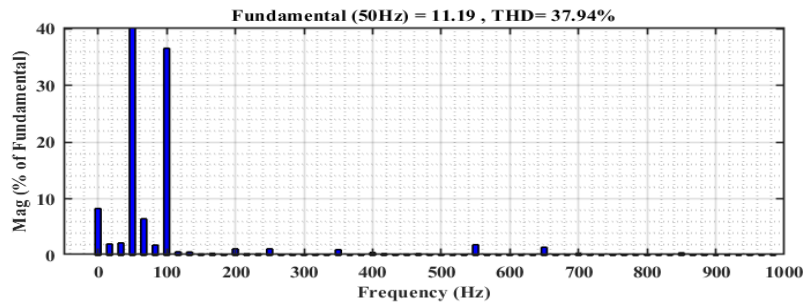


Fig.12. THD analysis at the inverter output

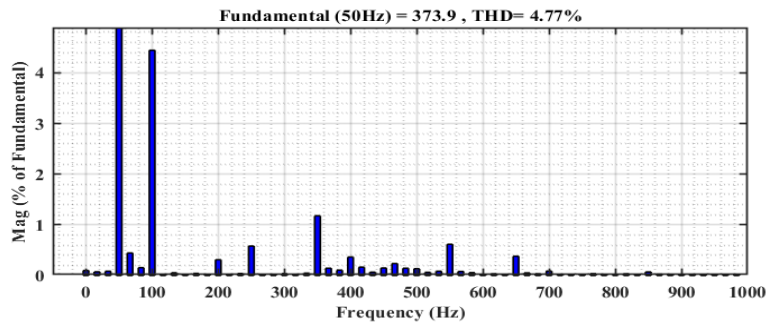


Fig.13. THD analysis of phase voltage  $V_a$  signal with LC filter

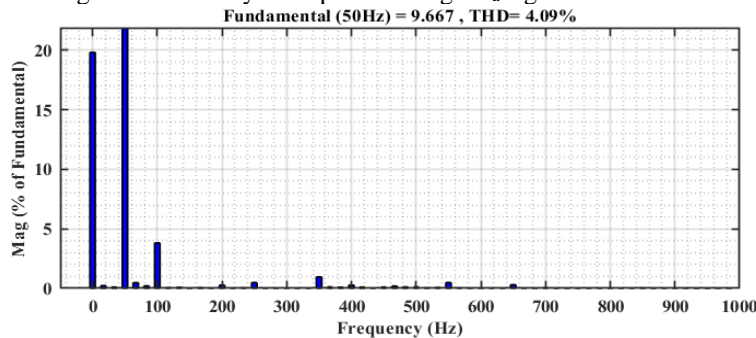


Fig.14. THD analysis of load current  $I_a$  of signal with LC filter



Table.3 THD with LC filter L=5mH, C=50uF at load side

Signals	THD%	Magnitude	Average % THD	IEEE std. 1547
V1	4.77	373.9 V	4.75	5%
V2	4.81	373.8 V		
V3	4.68	373.7V		
I1	4.09	9.67 A	4.05	
I2	4.12	9.67 A		
I3	3.96	9.67 A		

The waveform analyzed are current and voltage waveform Fig.11,12 and 13 respectively. Figure-11, shows the inverter THD analysis and has the THD in current waveform 37.94%. and current magnitude of 11.19 ampere. The THD analysis indicates that the voltage waveform of the three-phase system is relatively clean, with acceptable levels of harmonic distortion. This suggests that the system is operating within normal parameters and should not experience significant issues due to harmonic distortion. Table. 3 shows the THD analysis for load voltage and current signals which indicates better power quality. For reducing THD a three phase LC filter connected in between the load and inverter. THD can further reduced by increasing the size of LC filter.

**Conclusion:**

The Quasi ZSI converter topology demonstrated promising features for use in grid and utility applications. Its ability to provide boost and buck functionality, along with inherent impedance adaptation capability, makes it suitable for interfacing renewable energy sources like Solar PV to the grid. A robust control strategy developed to ensure optimal performance of the Quasi ZSI converter. The control scheme effectively regulated the output voltage, maintained maximum power point tracking (MPPT), and ensured grid integration compliance with minimal harmonic distortion. Results indicate better steady state and transient and rapid response to varying solar irradiance and load conditions, and improved power quality at the utility.

**APPENDIX**

The feed forward  $d_0$  can be calculated in equilibrium state by equation (1) [3].

$$d_0 = \frac{v_{C1}^* - v'_{in}}{2v_{C1}^* - v'_{in}} \tag{1}$$

Types of transfer function used in simulation

$$G_{\hat{d}_0}^{i_L}(s) = \left. \frac{i_L(s)}{\hat{d}_0(s)} \right|_{\substack{i_{\text{rad}}(s)=0 \\ v_{in}(s)=0}} = \frac{(V_{C1} + V_{C2} - R I_{\text{load}})Cs - (I_{\text{load}} - I_{L1} - I_{L2})(1 - 2D_0)}{LCs^2 + C(r+R)s + (1 - 2D_0)^2} \tag{2}$$

$$G_{i_{\text{load}}}^{\hat{v}_C}(s) = \left. \frac{\hat{v}_C(s)}{i_{\text{load}}(s)} \right|_{\substack{\hat{d}_0(s)=0 \\ \hat{v}_{in}(s)=0}} = \frac{R(1 - D_0)(1 - 2D_0) - (1 - D_0)(Ls + r + R)}{LCs^2 + C(r+R)s + (1 - 2D_0)^2} \tag{3}$$

$$G_{i_{\text{load}}}^{i_L}(s) = \left. \frac{i_L(s)}{i_{\text{load}}(s)} \right|_{\substack{\hat{d}_0(s)=0 \\ \hat{v}_{ic}(s)=0}} = \frac{R(1 - D_0)Cs + (1 - D_0)(1 - 2D_0)}{LCs^2 + C(r+R)s + (1 - 2D_0)^2} \tag{4}$$

Table-1. Comparison of boosting methods in QZSI

Methods	M & D <sub>0</sub> expression	V <sub>p-p</sub> Voltage at Capacitor
Simple Boost	$M \leq (1 - D_0)$	$v_{c1} \geq 2v_{p-p}$
Maximum Constant Boost	$M \leq \frac{2}{\sqrt{3}}(1 - D_0)$	$v_{c1} \geq \sqrt{3}v_{p-p}$
Maximum Boost	$M \leq \frac{2\pi}{3\sqrt{3}}(1 - D_0)$	$v_{c1} \geq 1.65v_{p-p}$

## References

- [1] D. Vinnikov and I. Roasto, "Quasi-Z-Source-Based Isolated DC / DC Converters for Distributed Power Generation," *IEEE Trans. Ind. Electron.*, vol. 58, no. 1, pp. 192–201, 2011, doi: 10.1109/TIE.2009.2039460.
- [2] E. Engineering and Q. I. Circuit, "Quasi-Z-Source Inverter for Photovoltaic Power Generation Systems," *2009 Twenty-Fourth Annu. IEEE Appl. Power Electron. Conf. Expo.*, pp. 918–924, 2009, doi: 10.1109/APEC.2009.4802772.
- [3] Y. Li, S. Jiang, S. Member, and J. G. Cintron-rivera, "Modeling and Control of Quasi-Z-Source In- verter for Distributed Generation Applications," no. c, 2012.
- [4] F. Z. Peng, "Z-Source Inverter," *Conf. Rec. 2002 IEEE Ind. Appl. Conf. 37th IAS Annu. Meet. (Cat. No.02CH37344)*, vol. 2, pp. 775–781 vol.2, 2002, doi: 10.1109/IAS.2002.1042647.
- [5] Y. Li, "AC Small Signal Modeling , Analysis and Control of Quasi-Z-Source Converter," pp. 1848–1854, 2012.
- [6] Y. Tang, S. Xie, C. Zhang, and A. Z. V. Stress, "An Improved Z -Source Inverter," vol. 26, no. 12, pp. 3865–3868, 2011, doi: 10.1109/TPEL.2009.2039953.
- [7] M. Reza *et al.*, "High Gain Quasi-Switched Boost Inverter with Optimal Performance Parameters," *IEEE Trans. Transp. Electrifi.*, vol. 6, no. 2, pp. 554–567, Jun. 2020, doi: 10.1109/TTE.2020.2984159.
- [8] M. Nguyen and Y. Choi, "Transactions on Power Electronics PWM Control Scheme for Quasi-Switched-Boost Inverter to Improve Modulation Index," vol. 8993, no. c, 2017, doi: 10.1109/TPEL.2017.2717487.
- [9] W. Liu, Y. Pan, and Y. Yang, "Small-Signal Modeling and Dynamic Analysis of the Quasi-Z-Source Converter," *IECON 2019 - 45th Annu. Conf. IEEE Ind. Electron. Soc.*, vol. 1, pp. 5039–5044.
- [10] S. A. Singh, S. Member, G. Carli, and N. A. Azeez, "of a Modified Z-source Integrated PV / Grid / EV DC Charger / Inverter," vol. 0046, no. c, 2017, doi: 10.1109/TIE.2017.2784396.
- [11] T. S. Reddy, "A New Multilevel Z-Source Inverter for Distributed Generation," pp. 1573–1581.
- [12] Y. Huang, M. Shen, S. Member, F. Z. Peng, and J. Wang, "Z -Source Inverter for Residential Photovoltaic Systems," vol. 21, no. 6, pp. 1776–1782, 2006.
- [13] Y. Gu, Y. Chen, B. Zhang, and S. Member, "Enhanced-Boost Quasi-Z-Source Inverter with An Active Switched Z-Network," vol. 0046, no. 1, 2017, doi: 10.1109/TIE.2017.2786214.
- [14] F. Z. Peng, M. Shen, and Z. Qian, "Maximum boost control of the Z-source inverter," no. I, pp. 255–260, 2004.
- [15] E. Akbari, A. Zare, and G. Seyyedi, "Power quality enhancement of distribution grid using a photovoltaic based hybrid active power filter with three level converter," *Energy Reports*, vol. 9, pp. 5432–5448, 2023, doi: 10.1016/j.egy.2023.04.368.
- [16] F. Z. Peng, J. G. Cintron-rivera, and S. Jiang, "Controller Design for Quasi-Z-Source Inverter in Photovoltaic Systems," pp. 3187–3194, 2010.
- [17] J. Liu, J. Hu, and L. Xu, "Dynamic Modeling and Analysis of Z Source Converter — Derivation of AC Small Signal Model and Design-Oriented Analysis," vol. 22, no. 5, pp. 1786–1796, 2007.